



ARTICLE

Inhibition of AXL enhances chemosensitivity of human ovarian cancer cells to cisplatin via decreasing glycolysis

Min Tian^{1,2}, Xi-sha Chen¹, Lan-ya Li^{1,2}, Hai-zhou Wu^{1,2}, Da Zeng³, Xin-luan Wang⁴, Yi Zhang⁵, Song-shu Xiao³ and Yan Cheng¹

Anexelektin (AXL), a member of the TYRO3-AXL-MER (TAM) family of receptor tyrosine kinases (RTK), is overexpressed in varieties of tumor tissues and promotes tumor development by regulating cell proliferation, migration and invasion. In this study, we investigated the role of AXL in regulating glycolysis in human ovarian cancer (OvCa) cells. We showed that the expression of AXL mRNA and protein was significantly higher in OvCa tissue than that in normal ovarian epithelial tissue. In human OvCa cell lines suppression of AXL significantly inhibited cell proliferation, and increased the sensitivity of OvCa cells to cisplatin, which also proved by nude mice tumor formation experiment. KEGG analysis showed that AXL was significantly enriched in the glycolysis pathways of cancer. Changes in AXL expression in OvCa cells affect tumor glycolysis. We demonstrated that the promotion effect of AXL on glycolysis was mediated by phosphorylating the M2 isoform of pyruvate kinase (PKM2) at Y105. AXL expression was significantly higher in cisplatin-resistant OvCa cells A2780/DDP compared with the parental A2780 cells. Inhibition of AXL decreased the level of glycolysis in A2780/DDP cells, and increased the cytotoxicity of cisplatin against A2780/DDP cells, suggesting that AXL-mediated glycolysis was associated with cisplatin resistance in OvCa. In conclusion, this study demonstrates for the first time that AXL is involved in the regulation of the Warburg effect. Our results not only highlight the clinical value of targeting AXL, but also provide theoretical basis for the combination of AXL inhibitor and cisplatin in the treatment of OvCa.

Keywords: ovarian neoplasms; AXL; R428; tumor metabolism; Warburg effect; glycolysis; PKM2; cisplatin resistance

Acta Pharmacologica Sinica (2021) 42:1180–1189; <https://doi.org/10.1038/s41401-020-00546-8>

INTRODUCTION

The latest cancer statistics estimate that 21,750 new cases of ovarian cancer (OvCa) will be diagnosed and 13,940 patients will die of OvCa in the United States in 2020 [1]. Since the early symptoms of OvCa are atypical and there is no effective method for early diagnosis, OvCa is called the “invisible killer” of female health [2]. Patients with OvCa often initially respond to first-line platinum-based treatment (~70% of patients respond to therapy), but unfortunately, most of them experience relapse due to platinum resistance [3]. Poor chemotherapy sensitivity is one of the main causes of treatment failure, thus resulting in patient death from OvCa [4]. Although several pathways related to cisplatin resistance in OvCa have been reported [5], the underlying mechanisms remain to be further explored.

Recent data indicated that AXL, a member of the TAM family of RTK, is strongly upregulated and highly related to poor prognosis in OvCa [6]. It has been reported that AXL is highly expressed in a variety of malignant tumors and promotes tumor development in breast cancer [7, 8], NSCLC [9], melanoma [10], and prostate cancer [11]. AXL autophosphorylates at residues Y702 and Y703 after binding to ligand growth arrest specific 6 (Gas6) or dimerizing with other RTK extracellular domains [12]. The activation of AXL promotes the tyrosine phosphorylation of its

substrate protein, activates downstream pathways, accelerates tumor proliferation, epithelial-mesenchymal transition, and immune escape, and plays an important role in the development of cancer [13]. Several studies have reported that AXL plays a major role in tumor resistance to targeted therapies [14] and conventional cytotoxic agents, such as vincristine [15], etoposide [16], and cisplatin [17]. The study published by Jeanne M. *et al.* indicated that AXL promotes OvCa resistance to platinum drugs [18]. However, the underlying mechanism by which AXL regulates cisplatin resistance in OvCa needs to be further clarified.

The reprogramming of energy metabolism has been identified as a new characteristic of cancers in which most cancer cells generate energy by aerobic glycolysis instead of oxidative phosphorylation [19–21]. Aerobic glycolysis not only promotes cancer progression but also contributes to drug resistance, thereby decreasing the efficiency of anticancer therapies [22–25]. In the process of glucose metabolism, pyruvate kinase is the rate-limiting enzyme in the final step of the glycolytic pathway and catalyzes the conversion of phosphoenolpyruvate (PEP) and ADP into pyruvate and ATP [26]. PK consists of four isoforms, PKR, PKL, PKM1, and PKM2. PKM2, also called tumor-specific pyruvate kinase, is mainly expressed in tumor tissues [27]. PKM2 is considered to be a key factor affecting the prognosis of OvCa

¹Department of Pharmacy, The Second Xiangya Hospital, Central South University, Changsha 410011, China; ²Xiangya School of Pharmaceutical Sciences, Central South University, Changsha 410008, China; ³Department of Gynecology and Obstetrics, The Third Xiangya Hospital, Central South University, Changsha 410008, China; ⁴Translational Medicine R&D Center, Institute of Biomedical and Health Engineering, Shenzhen Institutes of Advanced Technology, Chinese Academy of Sciences, Shenzhen 518057, China and ⁵Department of Pharmacology, College of Pharmaceutical Sciences, Soochow University, Suzhou 215000, China
Correspondence: Song-shu Xiao (xiaosongshu@csu.edu.cn) or Yan Cheng (yancheng@csu.edu.cn)

Received: 13 February 2020 Accepted: 21 September 2020

Published online: 4 November 2020

by regulating glycolysis [28]. The inhibition of PKM2 can significantly inhibit the proliferation of OvCa cells with no obvious toxicity to mice, indicating that PKM2 is a potential therapeutic target for OvCa [29]. Analysis of the cisplatin-resistant COC1/DDP cell line and its parental COC1 cell line by LC-MS/MS also revealed that PKM2 contributes to cisplatin resistance in OvCa cells [30]. The phosphorylation of PKM2 at tyrosine 105 is a key site for the regulation of PKM2 activity, since it promotes aerobic glycolysis by inhibiting PKM2 activity [31]. It has been shown that the receptor tyrosine kinase FGFR1 phosphorylates the tyrosine (Y) 105 residue of PKM2 to inhibit its activity and promote the Warburg effect [32].

In this study, we demonstrated for the first time that the regulatory role of AXL in glycolysis is mediated by phosphorylating PKM2 in OvCa. The inhibition of AXL not only suppressed cell proliferation but also increased the sensitivity of parental cells and cisplatin-resistant OvCa cells to cisplatin. Overall, our study proposed that the combination of an AXL inhibitor and cisplatin will be an effective new strategy for OvCa therapy.

MATERIALS AND METHODS

Cell lines and culture

The human OvCa cell lines HO-8910 and SKOV3.ip were cultured in RPMI-1640 medium supplemented with 10% fetal bovine serum (Gibco, USA) and antibiotics (Biological Industries, Israel). The cisplatin-resistant human OvCa cell line A2780/DDP and its parental cell line A2780 were cultured in Dulbecco's modified Eagle's medium (DMEM)/high glucose medium supplemented with 10% FBS and antibiotics. HEK293T cells were cultured in DMEM supplemented with 10% FBS. The cells were maintained at 37 °C with 5% CO₂ in a humidified incubator.

Reagents and antibodies

R428 and 2-DG were purchased from Selleck. Cisplatin was purchased from Sigma-Aldrich. Rabbit monoclonal antibodies against AXL, PKM2, and phospho-PKM2 (Y105) were purchased from Cell Signaling Technologies. Anti-β-actin, anti-His, and anti-GST antibodies were purchased from Proteintech.

Plasmids and siRNA transfection

Gene silencing was performed for the OvCa cell lines in 6-well plates at 1.5×10^5 cells per well. The cells were transfected with commercially validated siRNAs (50 nM; siNT, siAXL, and siPKM2) were purchased from RiboBio, China) using Lipofectamine 2000 (Invitrogen, USA). The effective silencing of siRNA was determined by protein expression, and all experiments with gene silencing were performed 48–96 h after transfection. For plasmid transfection, the cells were transfected with a mixture of His-AXL, GST-PKM2 plasmid (Vigene Biosciences, China) or empty vector and Lipofectamine 2000. The cells were incubated for 48 h after transfection before testing for transgene expression or performing subsequent experiments.

Generation of stable AXL knockdown cell lines

HO-8910 and SKOV3.ip cells grown in 6 cm dishes were transfected with lentiviruses harboring shNT or shAXL (Genechem, China). The resultant cell lines were selected with 2 μg/mL puromycin for 6–10 days. The knockdown efficiency was assessed by Western blotting.

RNA isolation and analysis of gene expression by RT-qPCR

Total RNA was isolated from OvCa cells or tissue samples using TRIzol reagent (Cwbiotech, China) according to the manufacturer's instructions. The quality, quantity, and integrity of RNA were measured using a NanoDrop 2000 spectrophotometer. A 20 μL reverse transcription reaction mixture including 1 μg of isolated RNA and an equal volume of primers and oligo dT was prepared using the TaqMan High-capacity cDNA Kit (Takara, Japan). SYBR[®]

Premix Ex TaqTM (Tli RNaseH Plus) (Takara, Japan) was used for real-time PCR, which was run on a Bio-Rad system. The 2^{-ΔΔCt} method was used to quantify gene expression. Actin served as an internal control relative to AXL. Primers were designed and synthesized by TsingKe Biotech.

Western blot analysis

The treated cells were washed with PBS and lysed by ice-cold RIPA buffer (Cwbiotech, China) supplemented with protease inhibitor cocktail and phosphatase inhibitor cocktail (Selleck, USA). A BCA protein assay kit (Beyotime, China) was used to quantify the protein concentration. The proteins (15–30 μg) were separated by 10% SDS-PAGE and transferred onto polyvinylidene difluoride (PVDF) membranes. The PVDF membranes were incubated with 5% skim milk prepared with 0.1% PBST (1 L PBS and 1 mL Tween 20) for 1 h at room temperature, followed by overnight incubation with primary antibodies at 4 °C. Subsequently, the membranes were washed with PBST and then incubated with anti-rabbit secondary antibody at room temperature for 1 h. Protein bands were visualized by chemiluminescence using ECL reagents, and β-actin was used as an internal control. Band intensities were analyzed using Image Lab software.

Immunoprecipitation

HEK293T cells transfected with His-AXL, GST-PKM2, or empty plasmids were harvested 48 h later and subjected to immunoprecipitation analysis. After extracting the protein lysate at 4 °C, a small amount of lysate was taken for WB analysis. Antibody 1 μg was added to the remaining supernatant and incubated at 4 °C for 1 h and then incubated with protein A/G plus agarose beads overnight. The protein-beads complex was washed four times with PBS buffer, resuspended in 30 μL of 1× SDS sample buffer, boiled for 5 min, and then resolved by 10% SDS-PAGE. The proteins were visualized by immunoblotting.

Determination of the levels of aerobic glycolysis

The cells were seeded at a density of 1.5×10^5 cells/well in a 6-well plate. Culture media was collected at 48 h after treatment, and the Glucose Kit (Robio, China) and Lactate Assay Kit (Jiancheng Bioengineering Institute, China) were used to determine the concentrations of glucose and lactate in the medium. The cells were seeded into 96-well plates at a density of 5×10^3 cells/well, and ATP production was determined 24 h later using an ATP assay kit (PerkinElmer, USA). Experiments were performed in triplicate.

Cell viability assay

Cell viability was examined using the Cell Counting Kit-8 (CCK-8) (Selleck, USA). At the end of the treatment, the cells were incubated with 10 μL of CCK-8 reagent in 5% CO₂ for 2 h at 37 °C. The result was detected at a wavelength of 450 nm.

5-Ethynyl-2'-deoxyuridine assay

The CellLightTM EdU Apollo R567 in vitro Imaging Kit (RiboBio, China) was used to observe the proliferation rate of cancer cells. At the end of the treatment, the cells were treated with 50 μmol/L EdU for 2 h at 37 °C. After fixation with 4% paraformaldehyde for 15 min, the cells were treated with 0.5% Triton X. The cells were incubated with 100 μL of 1× Apollo[®] reaction mixture for 30 min and then incubated with 5 μg/mL Hoechst 33342 for 30 min to stain the nucleus. The images were visualized under a fluorescence microscope.

Colony formation assay

The cells were seeded in 6-well plates at a low density (8×10^3 cells per well). After overnight incubation, the cells were treated with vehicle or drugs for 48 h, which were then replaced with conventional medium. The cells were then incubated for 14 days. Cell colonies were fixed with 4% paraformaldehyde for 30 min and

then stained with 0.1% crystal violet and photographed, after which the colonies were counted. Experiments were performed in triplicate.

Soft agar assay

SKOV3.ip cells stably transfected with shAXL or shNT were seeded on top of 1.2% agar in RPMI-1640 medium containing 10% FBS with 0.7% agar (Bioweste, Spain) in a 24-well plate. After 14 days, the clones were observed with a microscope and photographed. The clones from three independent experiments were quantified using ImageJ.

Tumor xenograft model

Subconfluent cultures of SKOV3.ip cells were washed with sterile PBS and resuspended at 2×10^7 cells/mL in PBS. Female athymic nude mice (aged 4–6 weeks) received 100 μ L of cell suspension via s.c. injection in the left or right flank. When the average tumor volume reached $>150 \text{ mm}^3$, the mice were randomly divided into four groups (5 mice per group) with the indicated treatments. The animals in the control group received the same volume of vehicle in the same way as the animals in the experimental group. The animals in the cisplatin treatment group received 1.2 mg/kg cisplatin intraperitoneally twice a week and were orally administered 0.1 mL of corn oil twice daily. The animals in the R428 treatment group received oral gavage of 7 mg/kg R428 twice a day and 0.1 mL of saline intraperitoneally twice a week. The animals in the cisplatin and R428 combination treatment group were administered 1.2 mg/kg cisplatin twice a week and 7 mg/kg R428 orally twice a day. The mice were weighed, and tumor diameters were measured with calipers every 2 days. Tumor progression was monitored by tumor size measurements every other day, and the tumor volume (V) was calculated using the following formula: $V = (W^2 \times L) \times \pi / 6$. On day 14 after administration, tumors were harvested, weighed, and photographed. All animal experimental procedures used in this study were approved by the Animal Ethics Committee of Central South University and conducted in accordance with the Guideline of the Care and Use of Laboratory Animals in Central South University.

Patient samples

With the approval of the Research Ethics Committee of the Third Xiangya Hospital of Central South University, high-grade epithelial OvCa samples were obtained. In addition, consent was received from all patients.

Statistical analysis

The data are presented as the mean \pm SD or mean \pm SEM of three independent experiments. Statistical analyses were performed by using the two-tailed unpaired Student's t test or two-way ANOVA as indicated in the corresponding figure legends. Differences were considered to be statistically significant at $P < 0.05$ ($P < 0.05$, $P < 0.01$).

RESULTS

AXL is a potential therapeutic target for the treatment of OvCa. To verify whether AXL plays an important role in the development of OvCa, we first analyzed the expression of AXL via public gene expression databases. The GSE14407 dataset from the GEO database, which contains the transcriptional expression profiles of OvCa, was analyzed (<https://www.ncbi.nlm.nih.gov/geo/>). The results demonstrated that AXL expression was significantly increased in epithelial OvCa samples compared to normal ovarian samples (Fig. 1a). We further examined the mRNA expression of AXL in OvCa patients and found that AXL was frequently (63.6%, 7/11) overexpressed in the tumor tissues compared with the contralateral normal ovarian tissues (Fig. 1b). The relevance of AXL to the clinical outcomes of OvCa patients was further analyzed

using survival analysis via PrognoScan (<http://www.prognoscan.org/>). As shown in Fig. 1c, the overall survival of patients with high AXL expression was significantly poorer than that of patients with low AXL expression ($P < 0.001$). Next, we measured AXL expression in OvCa cell lines and found that the expression of AXL in OvCa cells (HO-8910, A2780, and SKOV3.ip cells) was higher than that in ovarian epithelial cell line IOSE80 (Fig. 1d). The effect of AXL on the growth of OvCa cells was further explored. The CCK-8 assay showed that the cell proliferation rate was significantly reduced in OvCa cells with knockdown of AXL or AXL small-molecule inhibitor R428 treatment (Fig. 1e). Colony formation assays also showed that the colony-forming ability was significantly reduced in shAXL-SKOV3.ip cells compared with shNT-SKOV3.ip cells (Fig. 1f). We also explored the effect of AXL on anchorage-independent cell growth. The soft agar cloning experiment showed that the size and number of clones were significantly reduced after AXL silencing (Fig. 1g). These results indicate that AXL is related to the poor prognosis of OvCa patients and plays an important role in OvCa cell proliferation.

AXL promotes aerobic glycolysis in OvCa cells

To further explore the underlying mechanisms by which AXL promotes tumor progression, gene set enrichment analysis (GSEA) was used for pathway enrichment analysis. In addition to the known functions of regulating autophagy, apoptosis, and cell cycle (Supplementary Fig. 1), KEGG analysis showed that AXL was significantly enriched in the glycolysis pathways of cancer (Fig. 2a). To validate the results of pathway enrichment, the metabolic flux in OvCa cell lines with or without AXL knockdown was assessed by glucose consumption, lactate export, and ATP production. As presented in Fig. 2b, glucose consumption, lactate production, and ATP production were significantly decreased in AXL-silenced OvCa cells compared with the control cells. To further verify the regulatory role of AXL in glycolysis, we transfected A2780 cells with the His-AXL plasmid and measured glycolysis flux. A significant increase in glycolysis was observed in the cells after transfection with exogenous AXL (Fig. 2c). These results indicate that AXL increases the level of glycolysis in OvCa.

Based on the sequences of PKM2, we found that the Y105 position of PKM2 has the characteristics of an AXL phosphorylation motif, indicating that AXL may regulate the phosphorylation of PKM2 on tyrosine 105 (<http://gps.biocuckoo.cn/>). Western blot analysis revealed a significant decrease in the phosphorylation level of PKM2 at Y105 after transfection with siAXL, and there was no significant change in the level of PKM2 protein (Fig. 2d). To further illustrate the relationship between AXL and PKM2, a immunoprecipitation experiment was performed. Western blot analysis showed that AXL can be immunoprecipitated by the GST antibody and that PKM2 can also be immunoprecipitated by the His antibody, indicating that AXL interacts with PKM2 (Fig. 2e). The structural analysis of AXL and PKM2 showed that peptides 100–110 of PKM2 fit well with the catalytic domain of AXL, and the distance between the PKM2 Y105 residue and the γ -phosphate of ATP was $\sim 4.5 \text{ \AA}$, indicating that AXL can phosphorylate PKM2 at residue Y105 (Fig. 2f). We next tested whether AXL activates glycolysis through PKM2. The increase in glycolysis caused by AXL overexpression was blocked by PKM2 knockdown (Fig. 2g). Consistently, the suppression of glycolysis caused by AXL knockdown was rescued by PKM2 overexpression (Fig. 2h). These data together illustrate that AXL promotes the glycolysis of OvCa cells through PKM2.

AXL mediates the effect of cisplatin on aerobic glycolysis in OvCa cells

Several studies have reported that the upregulation of glycolysis is an important way for cancer cells to evade cisplatin-induced apoptosis [33], and glycolysis inhibition has been shown to increase the chemotherapeutic sensitivity of OvCa to cisplatin [34].

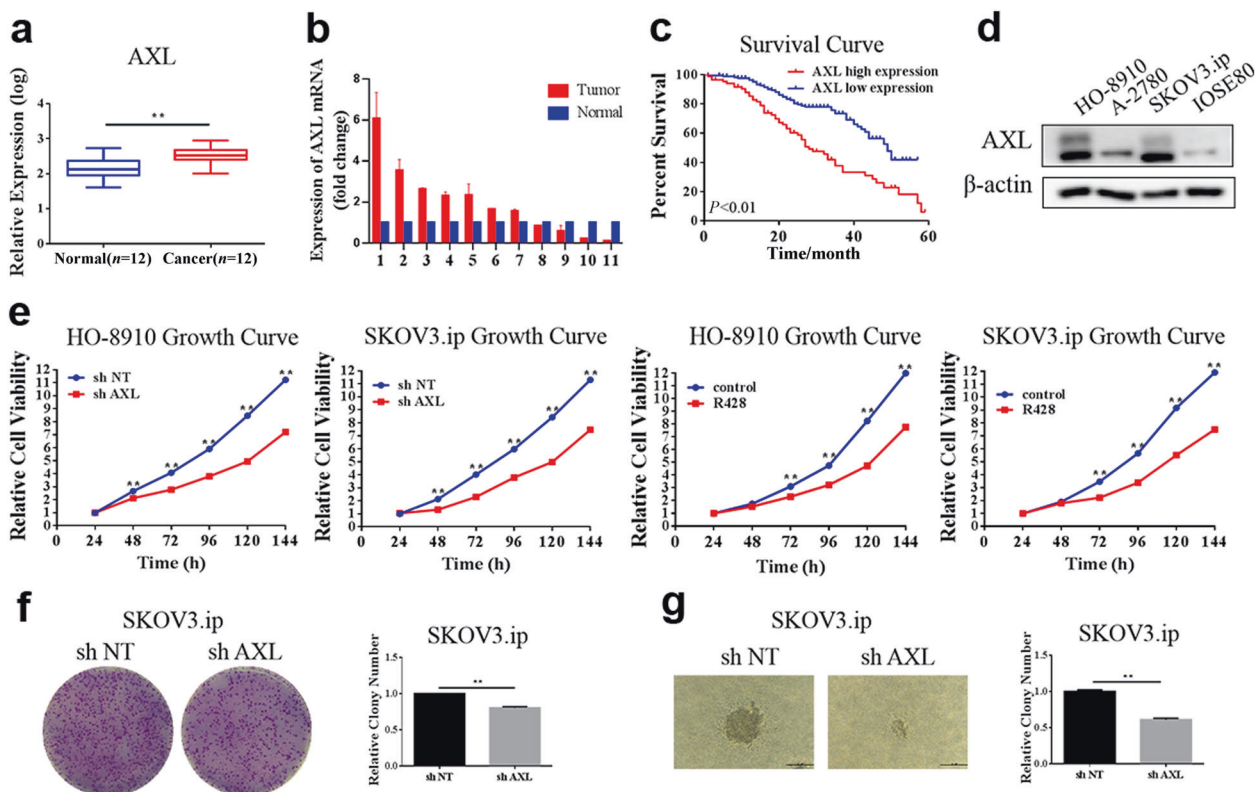


Fig. 1 AXL is a potential therapeutic target for the treatment of ovarian cancer. **a** GEO2R analysis comparing differences in AXL mRNA expression levels between normal ovarian epithelial tissue and OvCa tissue in GSE14407. **b** The levels of AXL mRNA between OvCa tissues and normal ovarian tissues were determined by qRT-PCR. Actin served as a loading control. **c** The effect of AXL mRNA levels on the overall survival of OvCa patients was analyzed in the GSE9891 dataset. **d** The expression of AXL protein in the normal ovarian epithelial cell line and OvCa cell lines was measured by Western blot analysis. Actin served as a loading control. **e** The cell proliferation of HO-8910 and SKOV3.ip cells stably transfected with shAXL or treated with 1 μ M R428 was measured by the CCK-8 assay. **f** Cell proliferation was measured by a colony formation assay in SKOV3.ip cells transfected with AXL shRNA. **g** SKOV3.ip-shNT and SKOV3.ip-shAXL cells were plated in 0.7% agar. After 14 days, colonies were photographed and quantified. ****** $p < 0.01$.

Consistent with those of previous studies, our results also show that cisplatin can promote glycolysis in a concentration-dependent manner in OvCa cells (Fig. 3a). In addition, we found that the combination therapy of cisplatin and the glycolysis inhibitor 2-DG had a stronger antitumor effect than cisplatin alone (Fig. 3b, c). Moreover, we also observed a concentration-dependent increase in AXL and p-PKM2 in cisplatin-treated OvCa cells (Fig. 3d), which prompted us to explore the role of AXL in the process of cisplatin-induced glycolysis. After silencing AXL, the induction of glycolysis by cisplatin was repressed (Fig. 3e), indicating that AXL mediates the regulation of glycolysis by cisplatin in OvCa cells. These results indicate that the increase in AXL expression may be the pro-survival mechanism of OvCa cells under cisplatin treatment.

Inhibition of AXL enhances the chemotherapy sensitivity of OvCa to cisplatin

Based on the above results, we further explored whether the inhibition of AXL could increase the sensitivity of OvCa cells to cisplatin. First, we used datasets from the Kaplan–Meier plotter (<http://kmpplot.com>) to analyze the relationship between AXL expression and the prognosis of patients with OvCa who received platinum chemotherapy. In patients receiving platinum chemotherapy, the survival time of the low AXL expression group was significantly longer than that of the high expression group (Fig. 4a), indicating that high AXL expression is associated with poor prognosis in patients treated with platinum chemotherapy. We further found that AXL expression was negatively correlated with the drug activity of cisplatin, which was illustrated by the

data of 7 OvCa cell lines from the Cell Miner Analysis Tool project (<http://discover.nci.nih.gov/cellminer/>) (Fig. 4b). Next, we demonstrated that silencing AXL increased the sensitivity of OvCa cells to cisplatin, as evidenced by CCK-8, colony formation, and EdU assays (Fig. 4c–e). These results suggest that silencing AXL promotes the chemosensitivity of OvCa cells to cisplatin. Moreover, the effect of AXL inhibition on enhancing cisplatin chemotherapy sensitivity was confirmed by using R428. As shown in Fig. 4f, g, combined treatment with cisplatin and R428 significantly enhanced the inhibitory effect of cisplatin on OvCa cells. Furthermore, the effect of AXL on cisplatin sensitivity in OvCa was determined in vivo. As shown in Fig. 5a–c, the combination of cisplatin and R428 was more effective in inhibiting tumor growth than either drug alone. In addition, the combination of R428 and cisplatin had no significant effect on the weight of mice (Fig. 5d). These results suggest that R428 has synergistic effects with cisplatin to promote the chemosensitivity of OvCa cells.

AXL is involved in cisplatin resistance in OvCa cells

To explore the reasons for the poor efficacy of cisplatin in some OvCa patients, ROC Plotter (<http://www.rocplot.org>), which divided the treated OvCa patients into responders and non-responders according to their pathological response [35], was used to compare the AXL gene expression levels between the two groups. Analysis of transcriptome data revealed that the expression level of AXL was related to the sensitivity of OvCa patients to cisplatin chemotherapy and that patients with no significant pathological response after platinum treatment had higher AXL expression levels (Fig. 6a). We further found that the mRNA level

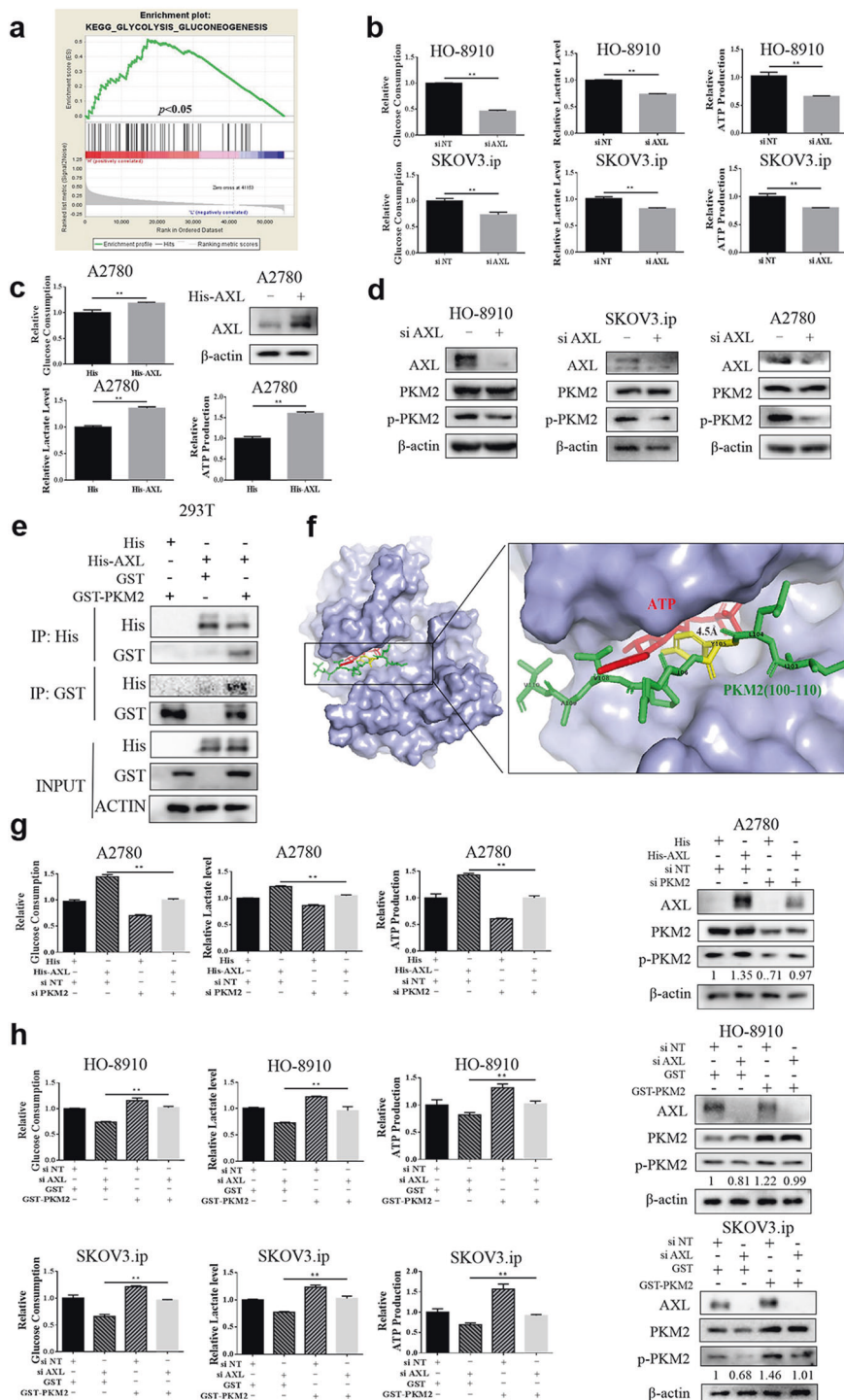


Fig. 2 AXL enhances aerobic glycolysis in ovarian cancer cells. **a** Enrichment plots from gene set enrichment analysis (GSEA) of AXL in glycolysis. **b** HO-8910 and SKOV3.ip cells were transfected with the nontargeting RNA or AXL siRNA and then tested for glucose uptake, lactate production, and ATP production. **c** A2780 cells transfected with the empty vector or His-AXL plasmid were tested for glucose uptake, lactate production, and ATP production. **d** HO-8910 and SKOV3.ip cells were transfected with nontargeting RNA or AXL siRNA, and the expression of AXL, PKM2, and p-PKM2 (Y105) was measured by WB. β -Actin served as a loading control. **e** HEK293T cells were transfected with His and GST-PKM2 plasmids, GST and His-AXL plasmids, or His-AXL and GST-PKM2 plasmids, followed by immunoprecipitation with anti-His and anti-GST antibodies. **f** Electrostatic surface view of AXL compounded with the PKM2 peptide. The close-up view shows that the PKM2 (100–110) peptide is suitable for the catalytic domain of AXL. The Y105 residue of PKM2 is highlighted in green, and the γ -phosphate of ATP is highlighted in red. **g** A2780 cells were transfected with either the nontargeting RNA or PKM2 siRNA, followed by transfection with a His-AXL plasmid, and then the expression of p-PKM2 and glycolysis level were measured. **h** HO-8910 or SKOV3.ip cells were transfected with nontargeting RNA or AXL siRNA, followed by transfection with the PKM2 plasmid. Then, the expression of p-PKM2 and glycolysis level were measured. $**P < 0.01$.

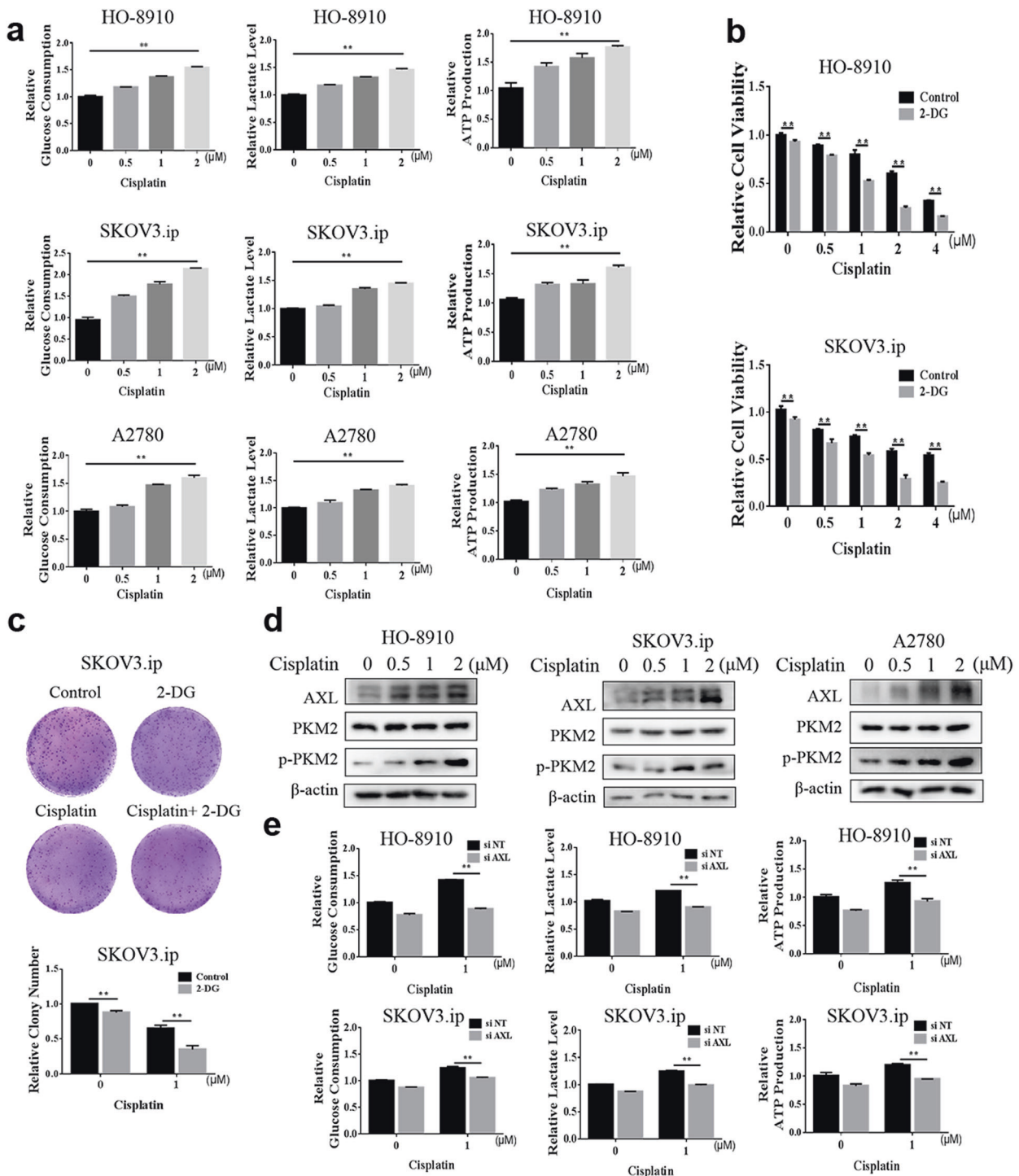


Fig. 3 **AXL is involved in cisplatin-regulated aerobic glycolysis in ovarian cancer cells.** **a** HO-8910, SKOV3.ip, and A2780 cells were treated with cisplatin, and glucose uptake, lactate production, and ATP production were measured. **b** HO-8910 and SKOV3.ip cells were treated with cisplatin in the presence or absence of 0.5 mM 2-DG. Cell viability was measured by the CCK-8 assay after 48 h. **c** SKOV3.ip cells were treated with 1 μ M cisplatin with or without 0.5 mM 2-DG, and cell proliferation was measured by the colony formation assay. **d** HO-8910, SKOV3.ip, and A2780 cells were treated with cisplatin; AXL, PKM2, and p-PKM2 protein expression was measured by WB; β -actin served as a loading control. **e** HO-8910 and SKOV3.ip cells were transfected with nontargeting RNA or AXL siRNA, followed by 1 μ M cisplatin treatment for 48 h, and then the glycolysis levels were measured. $^{***}P < 0.01$.

of AXL in the cisplatin-resistant OvCa cell line was significantly increased compared with that in the parental cell line using the GEO database (Fig. 6b). Compared to those in A2780 cells, the glycolysis levels and AXL and p-PKM2 expression were significantly higher in the A2780/DDP cisplatin-resistant OvCa cells

(Fig. 6c, d). These results suggest a potential role for AXL in regulating glycolysis and cisplatin resistance in OvCa. The silencing of AXL significantly decreased p-PKM2 expression and glycolysis levels in A2780/DDP cells (Fig. 6e, f). Consistently, the AXL inhibitor also reduced glucose consumption, lactate

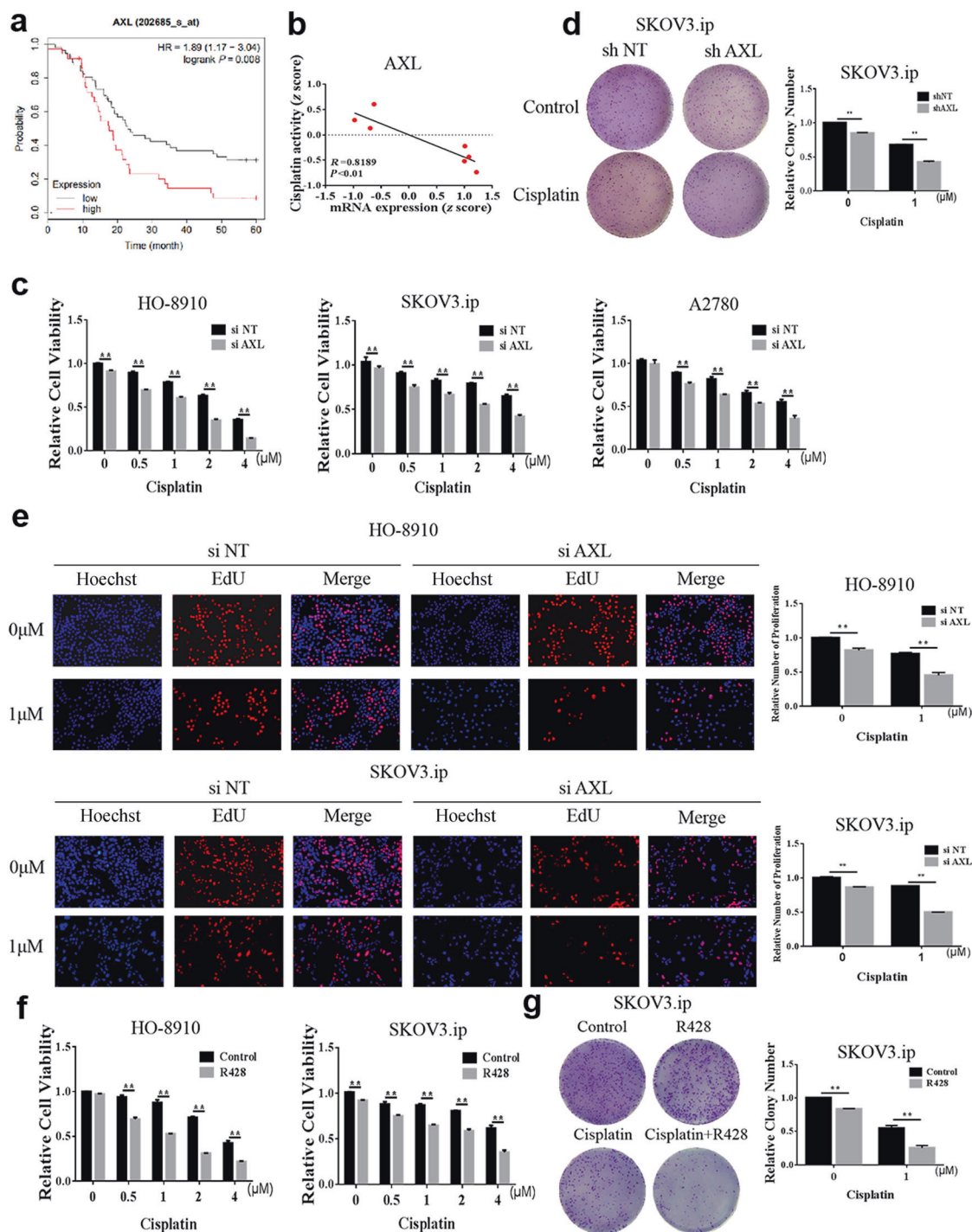


Fig. 4 AXL affects the chemotherapy sensitivity of ovarian cancer to cisplatin. **a** Kaplan–Meier curves for the PFS of 93 OvCa patients who received platinum as the chemotherapy drug (GSE26193). The patients were divided into two groups according to the level of AXL mRNA. **b** The mRNA expression of AXL in parent cells and cisplatin-resistant cells was compared in the GSE58470 dataset. **c** HO-8910, SKOV3.ip, and A2780 cells were transfected with AXL siRNA and then treated with cisplatin for 48 h, and cell viability was measured via the CCK-8 assay. **d** SKOV3.ip cells were transfected with AXL shRNA and treated with 1 μM cisplatin, and cell proliferation was measured by the colony formation assay. **e** HO-8910 and SKOV3.ip cells were transfected with AXL siRNA and then treated with 1 μM cisplatin for 48 h, and cell proliferation was assessed via the EdU assay. **f** HO-8910 and SKOV3.ip cells were pretreated with 1 μM R428 for 4 h and then treated with various concentrations of cisplatin. Cell viability was measured by the CCK-8 assay. **g** SKOV3.ip cells were pretreated with 1 μM R428 and then treated with 1 μM cisplatin, and cell proliferation was detected by the colony formation assay. ***P* < 0.01.

production, and ATP production levels in A2780/DDP cells (Fig. 6g), indicating the promotive effect of AXL on glycolysis in cisplatin-resistant OvCa cells. We further investigated whether AXL-mediated glycolysis affected the sensitivity of A2780/DDP cells

to cisplatin. As shown in Fig. 6h, i, A2780/DDP cells were more sensitive to cisplatin after silencing PKM2 or AXL. The CCK-8 assay also confirmed that the combination of the AXL inhibitor R428 and cisplatin (Fig. 6j) can significantly improve the therapeutic effect of

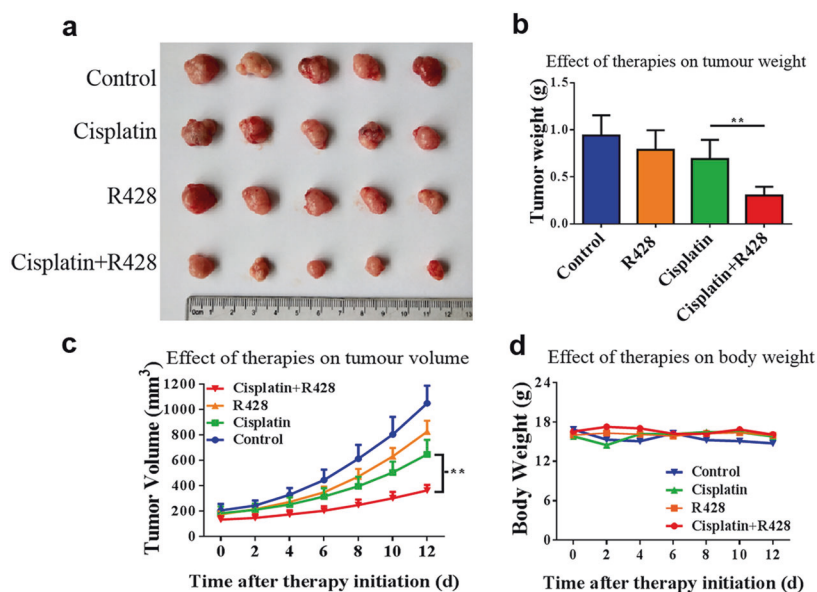


Fig. 5 Inhibition of AXL increases the cisplatin sensitivity of ovarian cancer *in vivo*. Four-week-old female nude mice were inoculated subcutaneously with SKOV3.ip cells. The tumor-bearing mice were grouped and received the indicated treatment. **a** Tumors were harvested and photographed at the termination of the experiment. **b** Tumor weights were measured after excision. **c** The average tumor volumes were measured every two days from the first day of administration. **d** Each mouse was weighed every 2 days. ****P** < 0.01.

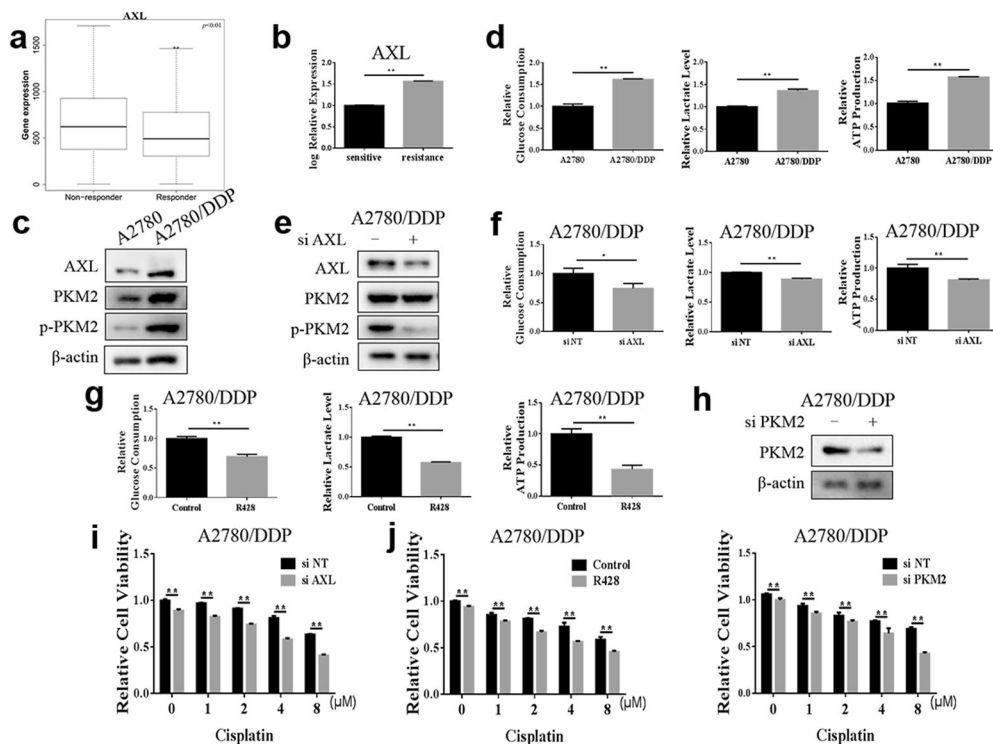


Fig. 6 Inhibition of AXL enhances the efficacy of cisplatin in chemoresistant ovarian cancer cells. **a** The ROC Plotter was used to analyze the transcriptome data of 961 patients, and the differences in AXL expression levels between patients with and without significant pathological response after platinum treatment were compared. **b** The mRNA expression levels of AXL in the parental cisplatin-sensitive IGROV-1 cell line and acquired cisplatin-resistant IGROV-1/Pt1 cell line were compared in GSE58470. **c** Western blotting detection of AXL, PKM2, and p-PKM2 expression in A2780 and A2780/DDP cells; β-actin was used as a loading control. **d** The glycolysis levels of A2780 and A2780/DDP cells were measured. **e** A2780/DDP cells were transfected with either the nontargeting RNA or AXL siRNA, and the expression of AXL, PKM2, and p-PKM2 was detected by Western blotting; β-actin was used as a loading control. **f** A2780/DDP cells were transfected with AXL siRNA, and the glycolysis level was measured. **g** A2780/DDP cells were pretreated with 1 μM R428, and the glycolysis level was measured. **h** A2780/DDP cells were transfected with either the nontargeting RNA or PKM2 siRNA, followed by treatment with cisplatin, and then cell viability was measured by the CCK-8 assay. **i** A2780/DDP cells were transfected with siNT or siAXL, followed by treatment with cisplatin, and cell viability was measured by the CCK-8 assay. **j** A2780/DDP cells were pretreated with 1 μM R428 for 4 h and then treated with cisplatin for 48 h. Cell viability was measured by the CCK-8 assay. ****P** < 0.01.

cisplatin in A2780/DDP cells. Altogether, these results indicate that AXL is involved in the acquired resistance of OvCa to cisplatin by promoting glycolysis, and the inhibition of AXL can significantly improve the therapeutic effect of cisplatin in chemoresistant cells.

DISCUSSION

The most common treatment for OvCa is surgery combined with chemotherapy. Cisplatin is widely used as a first-line treatment in the clinical treatment of OvCa [36]. However, data from the American Cancer Center indicated that the 5-year overall survival rate of OvCa has not significantly increased over the past 20 years [37], and most patients will develop acquired chemoresistance. As patients are in critical need of new treatment options that can enhance the effects of standard-of-care chemotherapy, further molecular characterizations and novel therapeutic targets need to be validated. Herein, our study not only revealed the promotive role of AXL in OvCa cell proliferation by regulating glycolysis by phosphorylating PKM2 but also demonstrated that the inhibition of AXL enhanced the efficacy of cisplatin against OvCa cells, even cisplatin-resistant OvCa cells.

The overexpression of AXL has been detected in multiple cancers, and its role in supporting tumorigenesis is well recognized [38–40]. Sun et al. reported that the mRNA levels of AXL in OvCa tissues were significantly higher than those in normal ovarian tissues [41]. Consistently, our study demonstrated that AXL is overexpressed in OvCa cell lines, and the inhibition of AXL significantly decreased cell proliferation, illustrating that AXL is a very promising clinical therapeutic target for OvCa.

Bemcentinib (R428), an oral selective AXL inhibitor developed by BerGenBio, is the first AXL-specific TKI to enter clinical trials. In non-small cell lung cancer, the company has completed clinical phase II trials of combination therapy with bemcentinib and erlotinib [42]. The combination treatment of bemcentinib with the PD-1 inhibitor pembrolizumab in non-small cell lung cancer [43] and triple-negative breast cancer has entered clinical phase II [42]. These clinical trial results suggest that R428 may be successfully marketed in the future and widely used in antitumor therapy. Our research illustrated that combination with R428 can significantly promote the therapeutic effect of cisplatin in OvCa, which will be a new strategy to reduce the clinically applied concentration of cisplatin and improve the chemosensitivity of patients. It has been reported that AXL supports tumor growth and spread by regulating cell survival, proliferation, migration, and tumor microenvironment [44]. Our study found that the knockdown of AXL expression reduced glucose uptake and lactate production in OvCa cells, suggesting that AXL promotes glycolysis in tumors. The results provide new ideas for further studying the molecular mechanisms of AXL in affecting tumor development. Based on the characteristics of AXL as a receptor tyrosine kinase, we supposed that AXL may affect tumor progression by regulating the phosphorylation of the tyrosine sites of glycolysis-related enzymes. By studying the mechanism of AXL in regulating cancer metabolism, we demonstrated the regulatory effect of AXL on PKM2 for the first time. Our results provide evidence that AXL regulates PKM2 activity by interacting with PKM2 and phosphorylating it at the Y105 site. This interaction contributed to a decrease in the ability of PKM2 to bind to PEP, thereby promoting the glycolysis of OvCa cells. The molecular mechanism between AXL and PKM2 not only defined the new tyrosine kinase affecting PKM2 activity but also identified a new substrate protein for AXL.

Several papers have examined the relationship between AXL expression and chemoresistance in cancer cells [45–49]. AXL is considered to be associated with chemotherapy resistance in OvCa. For example, apigenin can significantly inhibit the growth of chemotherapy-resistant OvCa cells by inhibiting the expression of AXL [50]. Our results confirmed that the inhibition of AXL

significantly enhanced the sensitivity of OvCa cells to cisplatin. Importantly, the suppression of AXL reversed the resistance of OvCa cells to cisplatin. Deregulated cancer metabolism has been demonstrated to mediate therapeutic resistance due to increased energy production and metabolite synthesis, which promotes cell proliferation, decreases drug-induced apoptosis, and increases drug efflux [51, 52]. Our study confirmed that AXL promotes glycolysis in tumors, which affects the sensitivity of OvCa cells to cisplatin, suggesting that the effect on tumor metabolism may be a new direction for studying the relationship between AXL and chemotherapy resistance.

In conclusion, our study proposed that glycolysis is a new mechanism by which AXL promotes the development of tumors. Increased expression of AXL by cisplatin induced the phosphorylation of PKM2 and subsequently enhanced glycolysis, contributing to chemoresistance. Our results suggest that AXL could be a potential therapeutic target to improve the sensitivity of OvCa cells to cisplatin, providing a theoretical basis for the combination of R428 and cisplatin in the treatment of OvCa.

ACKNOWLEDGEMENTS

This work was supported by grants from the National Natural Science Foundation of China (No 81972480), and the Postgraduate Research and Innovation Project of Central South University (grant number: 2019zsts 769). A2780/DDP and A2780 cells were gifted by Pingan Ma (State Key Laboratory of Rare Earth Resource Utilization).

AUTHOR CONTRIBUTIONS

YC and MT conceived and designed the research. MT and DZ performed the experiments. MT, XSC, LYL, HZW, and DZ conducted the data analysis. SSX provided cell lines and clinical samples. MT drafted the manuscript. YC, XLW, YZ, and SSX revised and approved the manuscript.

ADDITIONAL INFORMATION

The online version of this article (<https://doi.org/10.1038/s41401-020-00546-8>) contains supplementary material, which is available to authorized users.

Competing interests: The authors declare no competing interests.

REFERENCES

1. Siegel RL, Miller KD, Jemal A. Cancer statistics, 2020. *CA: A Cancer J Clin.* 2020;70:7–30.
2. Coleman RL, Monk BJ, Sood AK, Herzog TJ. Latest research and treatment of advanced-stage epithelial ovarian cancer. *Nat Rev Clin Oncol.* 2013;10:211–24.
3. Liu J, Matulonis UA. New strategies in ovarian cancer: translating the molecular complexity of ovarian cancer into treatment advances. *Clin Cancer Res.* 2014;20:5150–6.
4. Vaughan S, Coward JI, Bast RC Jr., Berchuck A, Berek JS, Brenton JD, et al. Rethinking ovarian cancer: recommendations for improving outcomes. *Nat Rev Cancer.* 2011;11:719–25.
5. De Giorgi U, Casadei C, Bergamini A, Attademo L, Cormio G, Lorusso D, et al. Therapeutic challenges for cisplatin-resistant ovarian germ cell tumors. *Cancers (Basel).* 2019;11:1584.
6. Lozneanu L, Pinciroli P, Ciobanu DA, Carcangiu ML, Canevari S, Tomassetti A, et al. Computational and immunohistochemical analyses highlight AXL as a potential prognostic marker for ovarian cancer patients. *Anticancer Res.* 2016;36:4155–63.
7. Zhu C, Wei Y, Wei X. AXL receptor tyrosine kinase as a promising anti-cancer approach: functions, molecular mechanisms and clinical applications. *Mol Cancer.* 2019;18:153.
8. Meyer AS, Miller MA, Gertler FB, Lauffenburger DA. The receptor AXL diversifies EGFR signaling and limits the response to EGFR-targeted inhibitors in triple-negative breast cancer cells. *Sci Signal.* 2013;6:ra66.
9. Okimoto RA, Bivona TG. AXL receptor tyrosine kinase as a therapeutic target in NSCLC. *Lung Cancer (Auckl).* 2015;6:27–34.
10. Tworkoski KA, Platt JT, Bacchiocchi A, Bosenberg M, Boggon TJ, Stern DF. MERTK controls melanoma cell migration and survival and differentially regulates cell behavior relative to AXL. *Pigment Cell Melanoma Res.* 2013;26:527–41.
11. Paccetz JD, Vasques GJ, Correa RG, Vasconcellos JF, Duncan K, Gu X, et al. The receptor tyrosine kinase Axl is an essential regulator of prostate cancer

- proliferation and tumor growth and represents a new therapeutic target. *Oncogene*. 2013;32:689–98.
12. Myers SH, Brunton VG, Unciti-Broceta A. AXL inhibitors in cancer: a medicinal chemistry perspective. *J Med Chem*. 2016;59:3593–608.
 13. Vouri M, Hafizi S. TAM receptor tyrosine kinases in cancer drug resistance. *Cancer Res*. 2017;77:2775–8.
 14. Dunne PD, McArt DG, Blayne JK, Kalimutho M, Greer S, Wang T, et al. AXL is a key regulator of inherent and chemotherapy-induced invasion and predicts a poor clinical outcome in early-stage colon cancer. *Clin Cancer Res*. 2014;20:164–75.
 15. Keating AK, Kim GK, Jones AE, Donson AM, Ware K, Mulcahy JM, et al. Inhibition of Mer and Axl receptor tyrosine kinases in astrocytoma cells leads to increased apoptosis and improved chemosensitivity. *Mol Cancer Ther*. 2010;9:1298–307.
 16. Hong CC, Lay JD, Huang JS, Cheng AL, Tang JL, Lin MT, et al. Receptor tyrosine kinase AXL is induced by chemotherapy drugs and overexpression of AXL confers drug resistance in acute myeloid leukemia. *Cancer Lett*. 2008;268:314–24.
 17. Hong J, Peng D, Chen Z, Sehdev V, Belkhir A. ABL regulation by AXL promotes cisplatin resistance in esophageal cancer. *Cancer Res*. 2013;73:331–40.
 18. Quinn JM, Greenwade MM, Palisoul ML, Opara G, Massad K, Guo L, et al. Therapeutic inhibition of the receptor tyrosine kinase AXL improves sensitivity to platinum and taxane in ovarian cancer. *Mol Cancer Ther*. 2019;18:389–98.
 19. Hanahan D, Weinberg RA. Hallmarks of cancer: the next generation. *Cell*. 2011;144:646–74.
 20. Warburg O. On the origin of cancer cells. *Science*. 1956;123:309–14.
 21. Warburg O, Wind FEN. In metabolism of tumours. *J Gen Physiol*. 1927;8:519–30.
 22. Bhattacharya B, Mohd Omar MF, Soong R. The Warburg effect and drug resistance. *Br J Pharm*. 2016;173:970–9.
 23. Hua G, Liu Y, Li X, Xu P, Luo Y. Targeting glucose metabolism in chondrosarcoma cells enhances the sensitivity to doxorubicin through the inhibition of lactate dehydrogenase-A. *Oncol Rep*. 2014;31:2727–34.
 24. Zhang X, Ai Z, Chen J, Yi J, Liu Z, Zhao H, et al. Glycometabolic adaptation mediates the insensitivity of drug-resistant K562/ADM leukaemia cells to adriamycin via the AKT-mTOR/c-Myc signalling pathway. *Mol Med Rep*. 2017;15:1869–76.
 25. Zhou M, Zhao Y, Ding Y, Liu H, Liu Z, Fodstad O, et al. Warburg effect in chemosensitivity: targeting lactate dehydrogenase-A re-sensitizes taxol-resistant cancer cells to taxol. *Mol Cancer*. 2010;9:33.
 26. Wiese EK, Hitosugi T. Tyrosine kinase signaling in cancer metabolism: PKM2 paradox in the Warburg effect. *Front Cell Dev Biol*. 2018;6:79.
 27. Israelsen WJ, Dayton TL, Davidson SM, Fiske BP, Hosios AM, Bellinger G, et al. PKM2 isoform-specific deletion reveals a differential requirement for pyruvate kinase in tumor cells. *Cell*. 2013;155:397–409.
 28. Chao TK, Huang TS, Liao YP, Huang RL, Su PH, Shen HY, et al. Pyruvate kinase M2 is a poor prognostic marker of and a therapeutic target in ovarian cancer. *PLoS One*. 2017;12:e0182166.
 29. Talekar M, Ouyang Q, Goldberg MS, Amiji MM. Cosilencing of PKM-2 and MDR-1 sensitizes multidrug-resistant ovarian cancer cells to paclitaxel in a murine model of ovarian cancer. *Mol Cancer Ther*. 2015;14:1521–31.
 30. Chen X, Wei S, Ma Y, Lu J, Niu G, Xue Y, et al. Quantitative proteomics analysis identifies mitochondria as therapeutic targets of multidrug-resistance in ovarian cancer. *Theranostics*. 2014;4:1164–75.
 31. Christofk HR, Vander Heiden MG, Wu N, Asara JM, Cantley LC. Pyruvate kinase M2 is a phosphotyrosine-binding protein. *Nature*. 2008;452:181–6.
 32. Hitosugi T, Kang S, Vander Heiden MG, Chung TW, Elf S, Lythgoe K, et al. Tyrosine phosphorylation inhibits PKM2 to promote the Warburg effect and tumor growth. *Sci Signal*. 2009;2:ra73.
 33. Li FL, Liu JP, Bao RX, Yan G, Feng X, Xu YP, et al. Acetylation accumulates PFKFB3 in cytoplasm to promote glycolysis and protects cells from cisplatin-induced apoptosis. *Nat Commun*. 2018;9:508.
 34. Loar P, Wahl H, Kshirsagar M, Gossner G, Griffith K, Liu JR. Inhibition of glycolysis enhances cisplatin-induced apoptosis in ovarian cancer cells. *Am J Obstet Gynecol*. 2010;202:371 e1–8.
 35. Fekete JánosT, Györfy B. ROCplot.org: Validating predictive biomarkers of chemotherapy/hormonal therapy/anti-HER2 therapy using transcriptomic data of 3,104 breast cancer patients. *Int J Cancer*. 2019;145:3140–51.
 36. Jayson GC, Kohn EC, Kitchener HC, Ledermann JA. Ovarian cancer. *Lancet*. 2014;384:1376–88.
 37. Deborah K, Ronald D, Jamie N. NCCN Clinical Practice Guidelines in Oncology (NCCN Guidelines), Ovarian Cancer. <https://www.tri-kobe.org/> (2019).
 38. Rankin EB, Giaccia AJ. The receptor tyrosine kinase AXL in cancer progression. *Cancers (Basel)*. 2016;8:103.
 39. Paccez JD, Duncan K, Vava A, Correa RG, Libermann TA, Parker MI, et al. Inactivation of GSK3beta and activation of NF-kappaB pathway via Axl represents an important mediator of tumorigenesis in esophageal squamous cell carcinoma. *Mol Biol Cell*. 2015;26:821–31.
 40. Ou WB, Corson JM, Flynn DL, Lu WP, Wise SC, Bueno R, et al. AXL regulates mesothelioma proliferation and invasiveness. *Oncogene*. 2011;30:1643–52.
 41. Sun W, Fujimoto J, Tamaya T. Coexpression of Gas6/Axl in human ovarian cancers. *Oncology* 2004;66:450–7.
 42. US National Library of Medicine. ClinicalTrials.gov, <<https://clinicaltrials.gov/>> (2019).
 43. Linger RM, Cohen RA, Cummings CT, Sather S, Migdall-Wilson J, Middleton DH, et al. Mer or Axl receptor tyrosine kinase inhibition promotes apoptosis, blocks growth and enhances chemosensitivity of human non-small cell lung cancer. *Oncogene*. 2013;32:3420–31.
 44. Myers KV, Amend SR, Pienta KJ. Targeting Tyro3, Axl and MerTK (TAM receptors): implications for macrophages in the tumor microenvironment. *Mol Cancer*. 2019;18:94.
 45. Brand TM, Iida M, Stein AP, Corrigan KL, Braverman CM, Luthar N, et al. AXL mediates resistance to cetuximab therapy. *Cancer Res*. 2014;74:5152–64.
 46. Miller MA, Oudin MJ, Sullivan RJ, Wang SJ, Meyer AS, Im H, et al. Reduced proteolytic shedding of receptor tyrosine kinases is a post-translational mechanism of kinase inhibitor resistance. *Cancer Disco*. 2016;6:382–99.
 47. Konieczkowski DJ, Johannessen CM, Abudayyeh O, Kim JW, Cooper ZA, Piris A, et al. A melanoma cell state distinction influences sensitivity to MAPK pathway inhibitors. *Cancer Disco*. 2014;4:816–27.
 48. Elkabets M, Pazarentzos E, Juric D, Sheng Q, Pelosof RA, Brook S, et al. AXL mediates resistance to PI3Kalpha inhibition by activating the EGFR/PKC/mTOR axis in head and neck and esophageal squamous cell carcinomas. *Cancer Cell*. 2015;27:533–46.
 49. Wang C, Jin H, Wang N, Fan S, Wang Y, Zhang Y, et al. Gas6/Axl Axis contributes to chemoresistance and metastasis in breast cancer through Akt/GSK-3beta/beta-catenin signaling. *Theranostics*. 2016;6:1205–19.
 50. Suh YA, Jo SY, Lee HY, Lee C. Inhibition of IL-6/STAT3 axis and targeting Axl and Tyro3 receptor tyrosine kinases by apigenin circumvent taxol resistance in ovarian cancer cells. *Int J Oncol*. 2015;46:1405–11.
 51. Zhao Y, Butler EB, Tan M. Targeting cellular metabolism to improve cancer therapeutics. *Cell Death Dis*. 2013;4:532.
 52. Zhou Y, Tozzi F, Chen J, Fan F, Xia L, Wang J, et al. Intracellular ATP levels are a pivotal determinant of chemoresistance in colon cancer cells. *Cancer Res*. 2012;72:304–14.